MATERIALS PHYSICS AND MECHANICS RESEARCH ARTICLE

Submitted: March 21, 2026 **Revised: April 1, 2026** **Accepted: May 11, 2026**

Mechanical response of polyvinyl chloride under various stress triaxiality levels

T. Houari [1] ✉, H. Khellafi [1], E. Ould Chikh [1], H.M. Meddah [1], M. Bendouba [1], M. Benguediab [2]

[1] University Mustapha Stambouli, Mascara, Algeria

[2] University of Sidi Bel Abbes, Sidi Bel Abbe`s, Algeria

✉ tarek.houari@univ-mascara.dz

ABSTRACT

Polyvinyl chloride is a thermoplastic material commonly employed in various engineering applications. The material properties of polyvinyl chloride have been observed to vary significantly with the applied loading conditions. A comprehensive knowledge of the deformation and failure characteristics of the material is necessary for evaluating its performance in engineering applications. In the present work, the stress response of the material is studied by subjecting flat and notched polyvinyl chloride specimens of various geometries to uniaxial tensile testing. The tests were conducted at room temperature and over a range of strain rates, namely 10^{-3}, 10^{-2}, and 10^{-1} s^{-1}. In addition, tests were also conducted for a range of loading rates from 0.2 to 1.4 mm/s to explore the combined effect of strain rate and stress triaxiality. The results of the experiments indicate a three-stage deformation process of the material: viscoelastic deformation, necking and plastic flow, and a hardening process due to cavitation. An increase in the rate of strain results in an increase in the elastic modulus, yield strength, ultimate strength, and strain at fracture. The geometry of the test specimen also has a strong influence on the results. The effects of stress triaxiality and reduced ductility are related to the radius of curvature of the test specimen. The larger the radius of curvature of the test specimen, the more deformable the material. In addition, these results highlight the interaction between strain rate and stress state on the mechanical response and failure of polyvinyl chloride, providing a solid experimental basis for formulating models for the nonlinear elasto-viscoplastic response of the material.

KEYWORDS

polymeric materials • PVC • experimental characterization • uniaxial tension • plasticity • damage initiation elasto-viscoplastic behavior

Citation: Houari T, Khellafi H, Ould Chikh E, Meddah HM, Bendouba M, Benguediab M. Mechanical response of polyvinyl chloride under various stress triaxiality levels. *Materials Physics and Mechanics*. 2026;54(3): 120–136. http://dx.doi.org/10.18149/MPM.5432026_10

Introduction

The industrial development of polymers, commonly known as plastics, has seen significant growth since the last century, making their mechanical behavior a crucial area of research [1–3]. These materials are now widely used in various applications, with packaging being one of the largest consumers of plastic materials. In this research field, the problems related to the elasto-viscoplastic behavior of structures hold considerable technical importance, as they are essential for predicting the lifespan, safety, and reliability of components [4,5]. Recent experimental studies have therefore played a crucial role in characterizing the mechanical performance of polymers and their composites [6,7].

© T. Houari, H. Khellafi, E. Ould Chikh, H.M. Meddah, M. Bendouba, M. Benguediab, 2026.
Publisher: Peter the Great St. Petersburg Polytechnic University
This is an open access article under the CC BY-NC 4.0 license (https://creativecommons.org/li-censes/by-nc/4.0/)

In this context, several authors have investigated polymer behavior under different mechanical conditions. Reddy et al. [8] experimentally studied hybrid polymer composites and found that both tensile and flexural strengths increased with higher fiber content. Krishnaswamy [9] analyzed creep rupture failures in high-density polyethylene (HDPE) pipes, distinguishing between ductile and brittle modes and noting that ductile failure correlates with yield stress. Saad et al. [10] investigated PVC materials and found that gray PVC exhibited higher tensile strength than white PVC, and that yield stress increased with strain rate and decreased with temperature. Adams et al. [11] evaluated the mechanical properties of HDPE pipes for nuclear safety systems, providing key data on yield stress, modulus, and strain to support ASME code qualification.

In studies conducted between 2020 and 2025, researchers have extended their focus to even harder, more complex behaviors and materials. For example, Tang et al. [12] studied PVC-UH subjected to quasi-static strain rates by using digital image correlation (DIC), and their results showed five stages of deformation, all decreasing with an increase in strain rate. The researchers observed a linear increase in yield and fracture strength with respect to strain rate, whereas elongation decreases exponentially with respect to strain rate. This improved constitutive model of the material effectively predicts its response to various strain rates, thus improving the mechanical analysis of structures made from PVC-UH material. Kiass et al. [13] studied HDPE pipes, identifying three distinct stress–strain regions across their cross-section, with stress and modulus increasing from the external surface toward the internal surface of the pipes. Günöz et al. [14] studied the effect of seawater aging on glass fiber-reinforced epoxy pipes, where a constant reduction in hoop tensile strength was observed with time. Selini et al. [15] investigated the effect of stress triaxiality on the mechanical behavior of polyvinyl chloride (PVC) under plane stress conditions, combining experimental analysis with the G'Sell-Jonas phenomenological model. Their study focused on true stress–strain responses and highlighted the role of stress triaxiality and volumetric strain in plastic instability and fracture. Mesbah et al. [16] studied how stress triaxiality influences plastic deformation in high-density polyethylene, using a micromechanical model and experiments.

Tests on hourglass specimens revealed the interaction of plasticity and cavitation damage. The elastic-plastic-damage model was effective in explaining the influence of triaxiality on deformation and failure [17,18]. In a study by Benyahia et al. [19] on glass/epoxy pipes, higher temperatures reduce yield stress and stiffness but increase yield strain. El-Bagory et al. [20] also studied the mechanical behavior of HDPE pipes by testing dumbbell and ring specimens (notched and unnotched), cut at different angles and orientations. It was found that yield stress, necking, and fracture depend on geometry, strain rates, and fixtures. Notched ring specimens had higher yield stress. In addition, the effect of the crosshead speed was significant on the mechanical behavior of the specimens. It was also found that the test data are essential for designing HDPE pipes under different loading conditions [21–23]. Castagnet et al. [24] also studied the influence of microstructure and stress triaxiality on cavitation damage in semi-crystalline polymers. Annealing tests on specimens with different triaxialities revealed that annealing increased cavitation damage in weakly triaxial specimens but was insignificant in highly triaxial specimens. In highly triaxial specimens, hydrostatic stress dominates microstructure effects. Rahimidehgolan et al. [25] also studied the dynamic mechanical

behavior of PVC foams of different densities. In the experiment, a pneumatic test rig was developed to comply with the standards of ASTM D1621. It was found that a 35 % increase in plateau stress was observed at higher strain rates. In addition, a modified Nagy-Avalle model was effective in predicting the test data with an error of 1.7 %. It was also revealed that density-dependent rate sensitivity plateaus at a relative density of 0.125. Akel et al. [26] also studied the short- and long-term tensile behavior of PVC geomembranes at different strain rates. It was found that modulus, strength, and elongation at break decreased at low strain rates.

The novelty of this study lies in the combined experimental investigation of strain rate effects, stress triaxiality, and cavitation-driven damage in rigid PVC, a combination that has not been concurrently addressed in [27,28]. While several studies have examined the tensile behavior of PVC under uniaxial loading, most have focused either on rate sensitivity or on global mechanical properties, without considering the influence of multiaxial stress state or localized failure mechanisms. Unlike previous works that rely mainly on numerical modeling or monotonic testing, the present research provides direct experimental evidence of deformation localization, void nucleation, and fracture evolution under different geometrical constraints. This integrated approach offers original experimental data that can support future development of constitutive models and failure criteria for amorphous polymers, particularly in safety-critical applications [29,30].

The present study proposes a clear path for the experimental determination of the behavior of PVC when subjected to uniaxial tension. In this regard, tests were conducted on flat specimens at three distinct strain rates (10^{-3}, 10^{-2}, and 10^{-1} s^{-1}) to characterize the constitutive behavior of the material. Further tests were carried out under loading rates of 0.2, 0.6, 1.0, and 1.4 mm/s, along with flat and axisymmetrically notched specimens, which contribute to the understanding of the behavior of the material under different rates and how triaxial stress plays a role. This study examines the impact of strain rate on yield strength and elastic modulus, as well as the effects of specimen curvature on ductility.

The novelty of the present study lies in the experimental determination of the effect of strain rates, loading rates, and triaxial stress on the material. The present study offers fresh insights into the behavior of the material and forms a solid base for the determination of the constitutive model. Note that the present study is purely experimental and does not aim at developing a constitutive model.

Materials and Methods

Polyvinyl chloride (PVC) is a widely used thermoplastic polymer obtained by the polymerization of vinyl chloride. It is valued in engineering applications for its high rigidity, good chemical resistance, and durability [31,32]. Depending on formulation, its tensile stress at break typically ranges from 30–60 MPa for unplasticized PVC and from 10–25 MPa for plasticized PVC, with biaxially oriented unplasticized PVC reaching up to 90 MPa. These mechanical properties, combined with its low cost and ease of processing, explain its widespread use in pipe systems for water and drainage networks.

PVC pipes in service are subjected to combined stresses arising from internal pressure and soil interaction. While the circumferential stress is typically dominant, the axial stress can also become significant and, in certain conditions, may exceed the

circumferential stress. Accordingly, axial tensile and compression tests were carried out in this study to obtain a more comprehensive understanding of the pipe's mechanical behavior under realistic loading conditions.

Material preparation and specimens

The PVC investigated in this study was extracted from rigid pipes manufactured by STPM Mansouri Sétif (Algeria) for underground drainage applications, produced in accordance with German standards DIN 8061/8062, *unplasticized polyvinyl chloride (PVC-U) pipes* [33]. The pipes had an external diameter of 500 mm, a wall thickness of 12.6 mm, and a length of 6 m. Specimens for tensile and axial compression tests were cut along the longitudinal direction of the pipe (Fig. 1). To minimize heterogeneity between the pipe's skin and core regions, 2 mm of material was removed from both the inner and outer pipe surfaces. The remaining central layer was considered microstructurally homogeneous.

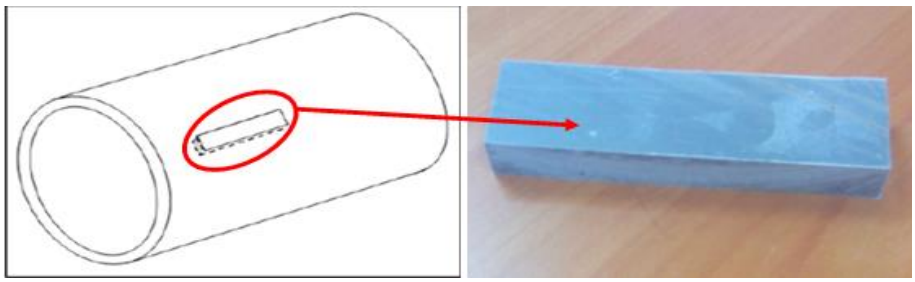


Fig. 1. Orientation of specimens cut from the longitudinal direction of the PVC pipe wall for tensile and compression tests

A total of 80 specimens were prepared from a single pipe using CNC machining (Emco Concept TURN 55 and MILL 55). Tensile specimens were prepared according to ASTM D638-14, *Standard Test Method for Tensile Properties of Plastics* (ASTM International, West Conshohocken, PA, USA, 2014) [34], with the following dimensions: thickness (b) = 2 mm, width (l) = 10 mm, and gauge length (L_0) = 40 mm (Fig. 2). For notched specimens, the gauge length (L_0 = 40 mm) was defined as the reduced section between the two curvature radii, where deformation is concentrated.

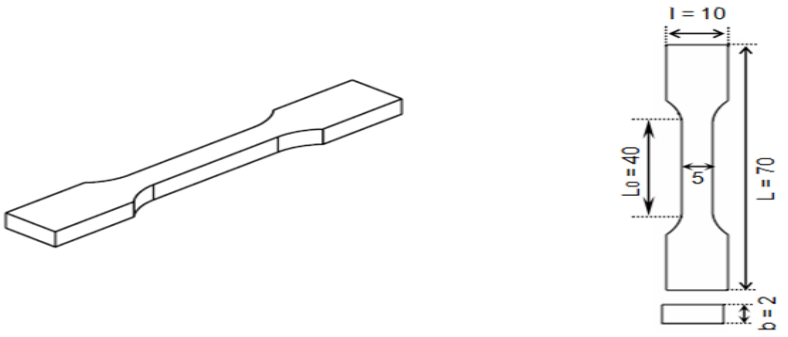


Fig. 2. Geometry of smooth tensile specimens

For each loading condition, four specimens were tested to ensure repeatability. The stress, train curves shown in the figures correspond to representative tests, while the reported mechanical properties were calculated using the arithmetic mean of the four measurements.

Geometry of notched axisymmetric and compression specimens

The specimens were extracted from PVC pipes with a diameter of 500 mm. Axisymmetric notched specimens (AE) with four different radii of curvature were selected to examine the impact of stress triaxiality on the material's behavior. The four radii of curvature considered were R = 80 mm (AE80), R = 10 mm (AE10), R = 4 mm (AE4), and R = 2 mm (AE2). Due to the specimen geometries, the overall length was 66 mm, the shank diameter was 10 mm, and the notch root diameter was 5 mm (Fig. 3). Each compression specimen had a cylindrical geometry with a length (L) of 6 mm and a diameter (d) of 6 mm, as shown in Fig. 4.

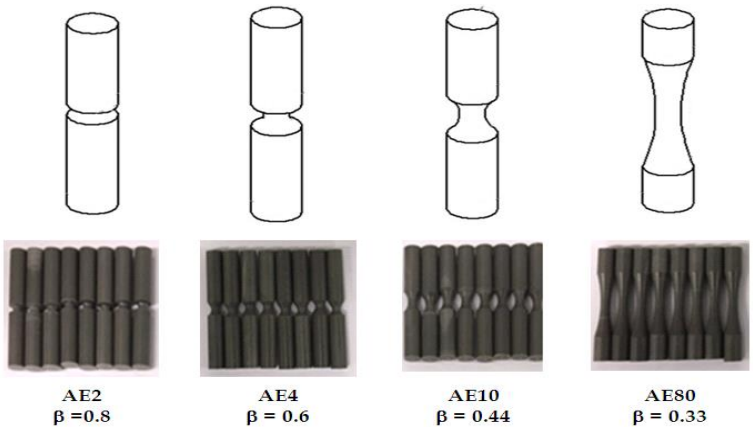


Fig. 3. Geometry of AE specimens

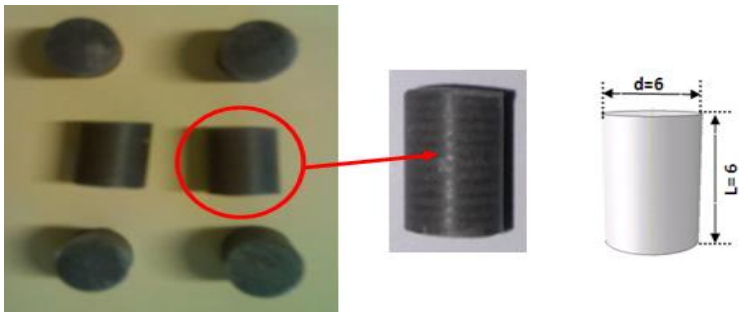


Fig. 4. Geometry of compression specimens

Tensile tests

Tensile tests were performed at ambient laboratory temperature (23 ± 2 °C) on an INSTRON 1341 hydraulic machine (Department of Polymers and Composites Technology, Mechanical Engineering, University of Mines, Douai, France). Two specimen geometries were tested: flat specimens prepared according to ASTM D638 M1A *(Standard Test Method for Tensile Properties of Plastics)* [33] and round axisymmetric notched specimens (AE).

Test conditions. Tests were carried out at three nominal strain rates (10^{-3}, 10^{-2}, and 10^{-1} s^{-1}) and corresponding crosshead speeds of 0.2, 0.6, 1.0, and 1.4 mm/s, consistent with those applied to AE specimens. Global displacement control was used, and crosshead displacement was recorded throughout the test. For flat specimens, three nominal strain rates were applied (10^{-3}, 10^{-2}, 10^{-1} s^{-1}). For notched specimens, four crosshead displacement speeds were used (0.2, 1.4 mm/s) to investigate the effect of triaxiality.

The engineering strain, ε, was computed by dividing the crosshead displacement by the gauge length of the specimen.

Strain measurement. Local strain fields were measured using two optical techniques:
1. A video-extensometer (video, traction system), consisting of a high-resolution camera linked to an image analysis system, was employed to monitor specimen deformation during loading.
2. Digital image correlation (DIC) was also utilized for full-field displacement capture and strains. Test surfaces were created by applying a thin coat of white paint, subsequently overlaid with a random black speckle pattern (Fig. 5).
3. The paint was applied immediately before testing to ensure proper adhesion and deformation with the specimen.
4. Flowchart of digital image correlation (DIC) method procedure which involves test record, file convert, software installation, Ncorr platform, strain computation method, DIC parameters setting, DIC processing analysis, calibration and scaling.
5. The tensile test video was recorded by the Nikon D3100 camera, which has a resolution of 4608 × 3072 pixels (14.2 effective megapixels).
6. It is noted that the strain accuracy and spatial resolution can be improved by increasing the resolution of the images to zome in the area of the specimen to be analyzed.
7. The Ncorr platform 1.1.2 version and Matlab R2017 version softwares are used in this study.
8. The Ncorr platform is recommended to use the Image Processing and Statistics Toolboxes, which runs the Ncoor program from Matlab R2017.
9. The aim of the image settings is to correlate and acquire the displacement/strain area of the specimen.

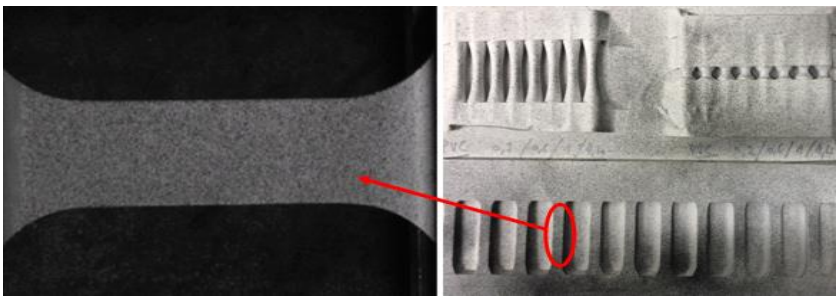


Fig. 5. Tensile specimen prepared with speckle pattern for DIC

No mechanical extensometer was used due to the large displacements involved in the tests. DIC analysis in this study was limited to longitudinal strain monitoring and damage localization. Transverse strain measurements were not included, as the primary focus was on axial deformation and cavitation onset under triaxial loading.

Compression tests

The tests for compression were carried out at the Lille Mechanics Laboratory, France. These tests were performed using a micro-machine (Deformation Devices System, Kammrath & Weiss). A 10 kN load cell was used to measure the applied force. The applied displacement rate was approximately 16 μm/s, resulting in a strain rate of $\dot{\varepsilon} = 2 \times 10^{-3}\ s^{-1}$. This value is of the same order of magnitude as the lowest strain rate used in tensile tests

(10^{-3} s^{-1}), ensuring consistency in the comparison of material behavior under tensile and compressive loading conditions. Cylindrical specimens with a height of 6 mm and a diameter of 6 mm were loaded between two parallel compression plates. To minimize friction effects, grease was applied to specimen faces that come into contact with the plates before testing (Fig. 6). All specimens were tested at room temperature (23 ± 1 °C).

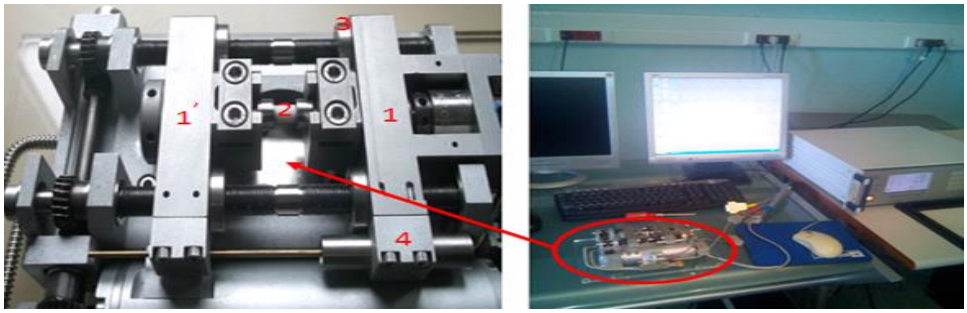


Fig. 6. Photograph of the mini-compression machine used. Legends: 1 and 1' - symmetrical crossheads; 2 - mini-specimen; 3 - motor; 4 - displacement sensor

Figure 7 presents the nominal stress-strain curve obtained from the compression test on PVC specimens. The stress was calculated using the initial cross-sectional area, and the strain was determined from the displacement measured over the initial height of the specimen. This curve reveals a typical response of an amorphous polymer, characterized by an initially linear elastic region followed by a progressive nonlinear viscoelastic behavior as the strain increases. Beyond approximately 10 % nominal strain, the material exhibits plastic deformation, with the stress reaching nearly 50 MPa.

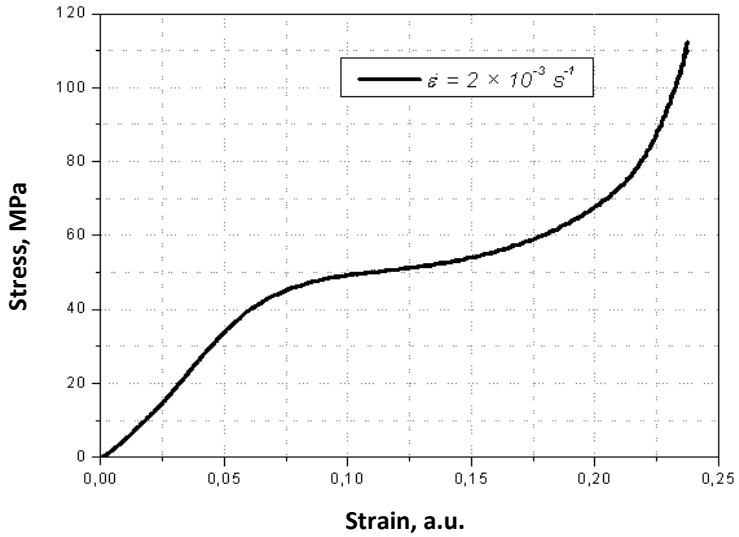


Fig. 7. Stress-strain curve of PVC in compression for a strain rate of $\dot{\varepsilon} = 2 \times 10^{-3}$ s^{-1}

From this response, it can be observed that PVC under compression displays an elastoplastic behavior, with an estimated Young's modulus of around 633 MPa and a nominal yield strength of about 40 MPa. These experimental observations provide valuable insight into the compressive mechanical behavior of PVC, without aiming to establish a constitutive model. Figure 8 shows the different compression specimens after loading.

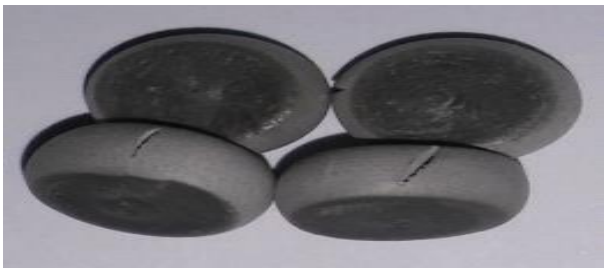


Fig. 8. Damaged compression specimens

Results and Discussion

Mechanical behavior

An experimental test was carried out to identify the constitutive behavior of PVC. From a plate, the specimen was removed, with geometry corresponding to the ASTM D638 M1A standard. The test was performed on an INSTRON tensile machine to work over a wide range of strain rates (10^{-3}, 10^{-2}, and 10^{-1} s^{-1}) at room temperature (23 °C).

Young's modulus (*E*) was determined graphically from the elastic slopes of the tensile curves. In finite element calculations, the chosen elastic modulus will be the apparent modulus. Mechanical parameters such as elastic modulus and yield stress were calculated as the arithmetic mean of four repeated tests. Experimental scatter remained below 7 %, confirming the repeatability of the measurements.

Poisson's ratio was determined from the slope of the longitudinal strain versus lateral strain curve on the same specimens. In the zone where the strain remains homogeneous (before necking), the average Poisson's ratio value is 0.4.

Just like the graphical determination of Young's modulus (*E*), the graphical determination of σ_0 poses serious precision problems on the nominal stress-strain curve. The stress σ_0 represents the boundary between the perfectly elastic domain and the onset of plasticity. Determining this barrier is challenging due to the presence of viscosity.

The different elastoplastic properties of the studied material can be derived from the stress-strain curves shown in Fig. 9, which illustrates the experimental stress–strain curves of PVC obtained under uniaxial tensile loading at three distinct strain rates (10^{-3}, 10^{-2}, and 10^{-1} s^{-1}). These curves, which illustrate the typical behavior at room temperature and under slow uniaxial loading of a semi-crystalline polymer, show three main zones:

Zone I: at the start of the curve shows a high, quasi-linear slope at the origin. This part is called the viscoelastic response. Softening is almost absent, and the yield point shows a gradual, rounded transition.

Zone II: the deformation becomes irreversible. Necking develops. This stage is partly associated with the unfolding of macromolecules under the applied deformation. The necking stabilizes, and the minimum diameter of the specimen hardly decreases. The neck and shoulders then propagate toward the ends of the specimen. This propagation results in a slight variation in force.

Zone III: this stage, referred to as the onset of structural hardening, is likely related to the orientation of chains along the main deformation direction. An increase in volume was linked to the formation and growth of cavities, leading to sudden rupture.

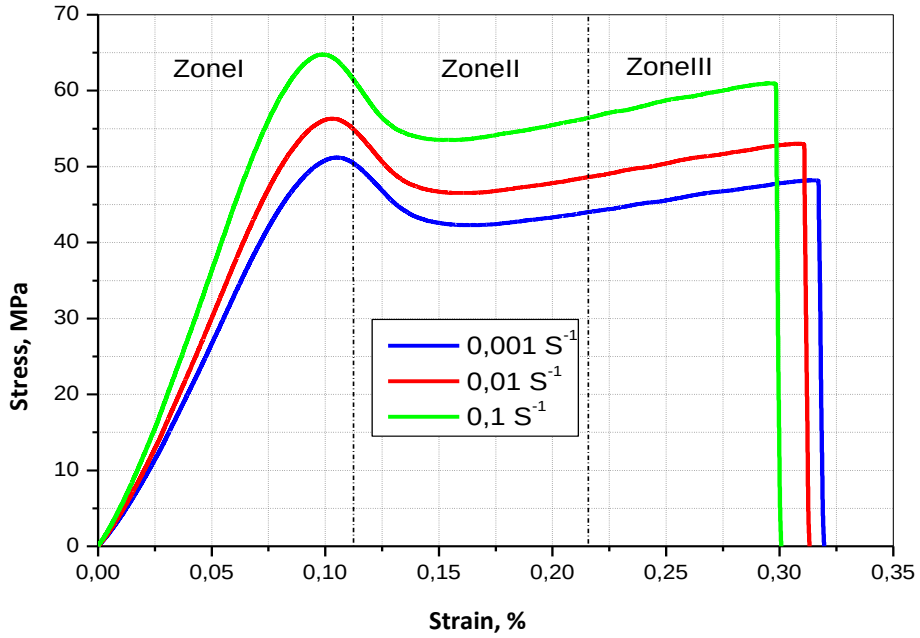


Fig. 9. Experimental stress–strain curves of PVC obtained from tensile tests at different strains

Figure 10 illustrates the fluctuation of the elastic modulus depending on the strain from experimental tests. Tensile tests at different strains provide information on the nature of polymers. For the same behavior, the yield strength and elastic modulus increase with the strain.

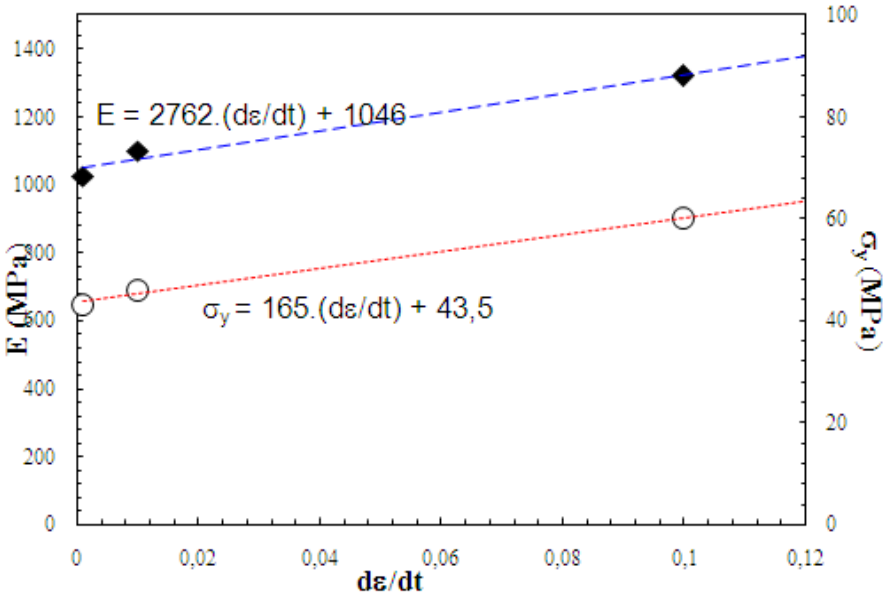


Fig. 10. Variation of the yield strength and elastic modulus in relation to strain rate

Effect of loading rate for flat specimens

Figure 11 shows true stress-true strain curves for tensile tests of flat specimens at different loading rates (0.2, 0.6, 1, and 1.4 mm/s). The stress escalates from (27.5 MPa) to a loading rate of (0.2 mm/s to 34 MPa at 1.4 mm/s). A similar pattern is evident for the

real strain, which rises from (1.18 to 1.92). True stress was computed from the current cross-sectional area, and true strain was calculated as the logarithm of the ratio between current and initial gauge lengths. This study concludes that true stress and true deformation increase with increasing loading rates. Figure 12 shows the different flat specimens after loading. The fracture of these specimens is localized in the gauge section.

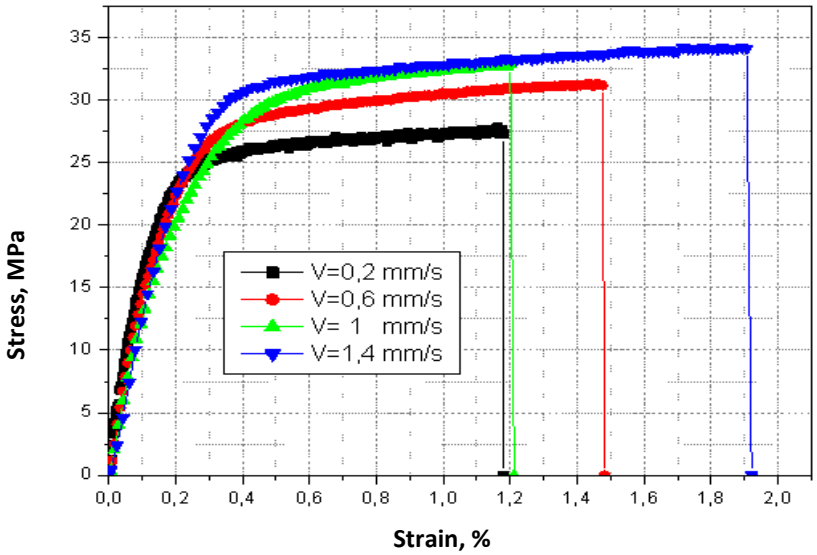


Fig. 11. The actual stress-strain curves for various loading rates



Fig. 12. Damaged flat tensile specimens

Effect of loading rate for different radii of curvature

Figure 13 shows true stress-true deformation curves taken at the critical point of the specimen for the four radii of curvature (0.33 for AE80, 0.44 for AE10, 0.6 for AE4, and 0.8 for AE2) and for the four loading rates (0.2, 0.6, 1, and 1.4 mm/s). The results highlight a strong dependence of behavior on this parameter. Thus, the elastic modulus and yield strength are affected by this parameter. Plastic flow, including plateau and hardening, is also affected by the loading rate. For a given specimen, the stress decreases with decreasing loading rate. In specimens AE2, AE4, AE10, and AE80, the maximum stress increases with increasing loading rates (0.2, 0.6, 1.0, and 1.4 mm/s). The deformation is low for a small radius of curvature (for the R = 2 mm specimen, the deformation does not exceed 0.15) and increases for a larger radius of curvature (for the R = 80 mm specimen, the deformation exceeds 0.4).

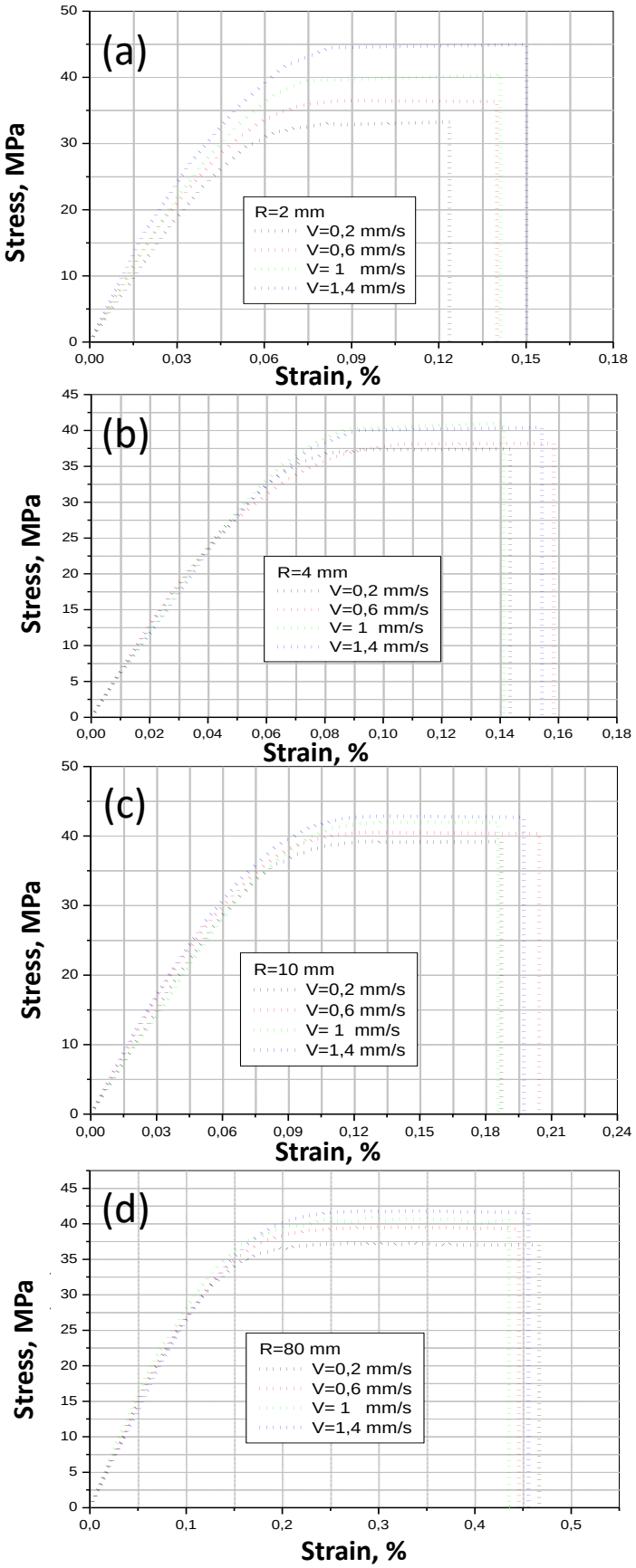


Fig. 13. Influence of loading rate on material behavior:
(a) R = 2 mm; (b) R = 4 mm; (c) R = 10 mm; (d) R = 80 mm

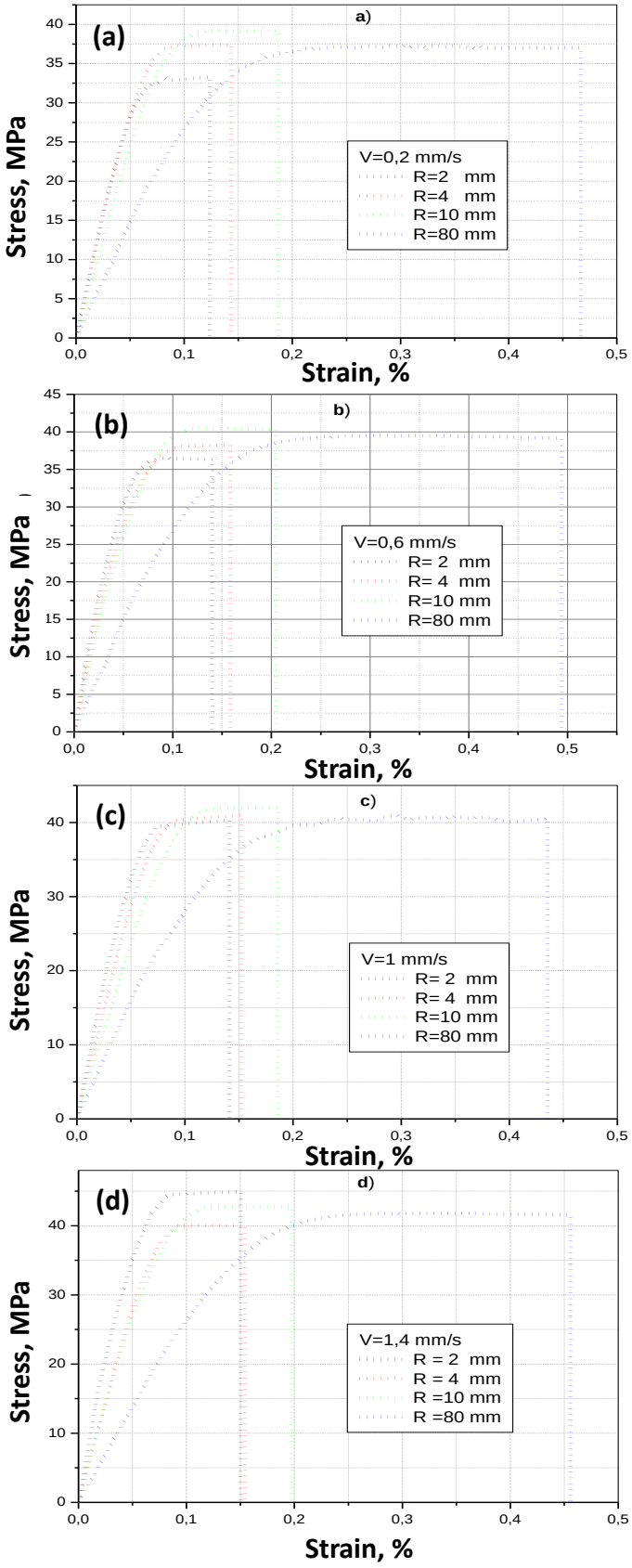


Fig. 14. Influence of radius of curvature on material behavior:
(a) V = 0.2 mm/s; (b) V = 0.6 mm/s; (c) V = 1 mm/s; (d) V = 1.4 mm/s

Effect of triaxiality on PVC behavior

Figure 14 illustrates the influence of radius of curvature on the tensile behavior of PVC specimens at different loading rates (0.2, 0.6, 1.0, and 1.4 mm/s). For lower loading rates (0.2, 0.6, and 1.0 mm/s), the yield strength generally increases with increasing radius of curvature for specimens AE2, AE4, and AE10, and a similar trend is observed for true strain. At the highest loading rate of 1.4 mm/s, the yield strength exhibits a non-monotonic behavior. Specifically, AE2 (R = 2 mm) shows a slightly lower yield strength than AE4 (R = 4 mm), indicating that the influence of triaxiality on yield strength depends on both loading rate and specimen geometry. For a radius of curvature of AE80, the true strain increases, unlike the cases of AE2, AE4, and AE10. This trend is due to the fact that PVC is soft and ductile under low triaxiality. The results reveal that the triaxiality ratio has a significant effect on the behavior of PVC.

Comparison with previous studies

The results obtained confirm the important effect of stress triaxiality on the mechanical behaviour of PVC. The stress-strain curves indicate that the radius of the notch root has a significant influence on the yield stress and true strain of the material. These results are in accordance with the work of Khellafi et al. [27], who found that the lower levels of triaxiality induced a more ductile behavior with larger plastic deformation and lower local stress concentration.

In the present study, the AE80 specimen exhibits higher true strain values than the AE2, AE4 and AE10 specimens, particularly at low loading rates. This behavior indicates that PVC has a better deformation ability under low triaxiality conditions. Similar findings were reported by Khellafi et al. [27], where low triaxiality resulted in a more stable plastic deformation with progressive strain hardening, while high triaxiality accelerated strain localization and damage initiation near the notch region.

Besides, at the highest loading rate (1.4 mm/sec), the results show a non-monotonic evolution of the yield stress, especially between AE2 and AE4 specimens. This observation confirms the fact that the mechanical response of PVC depends simultaneously on loading rate and specimen geometry according to the experimental and numerical results reported in the literature. In general, the comparison reveals a good agreement with previous studies and confirms the reliability of the adopted experimental approach to study the effect of triaxiality on PVC behavior.

Fracture surfaces

The fracture surface images were taken using a magnification device and software called Motic Images Plus 2.0 ML, a multimedia software offered by the Chinese group Motic Co., Ltd (Fig. 15). It is specially designed for individuals, providing advanced and easy-to-use methods for editing, analyzing, and measuring images.

Figure 16 shows fracture surfaces for some specimens from the tests performed. The surface morphology changes between the round specimens (R4, R80) and the flat specimen at a loading rate of 0.2 mm/s.

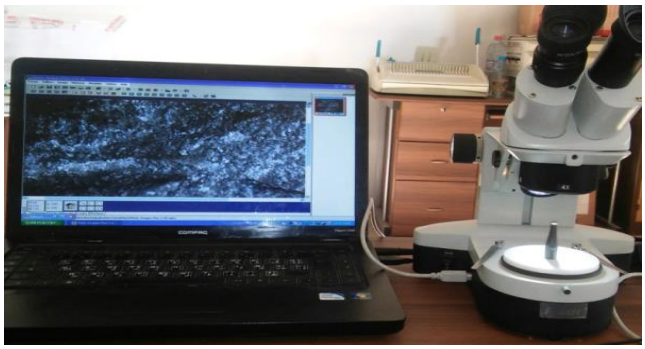


Fig. 15. Motic magnification device

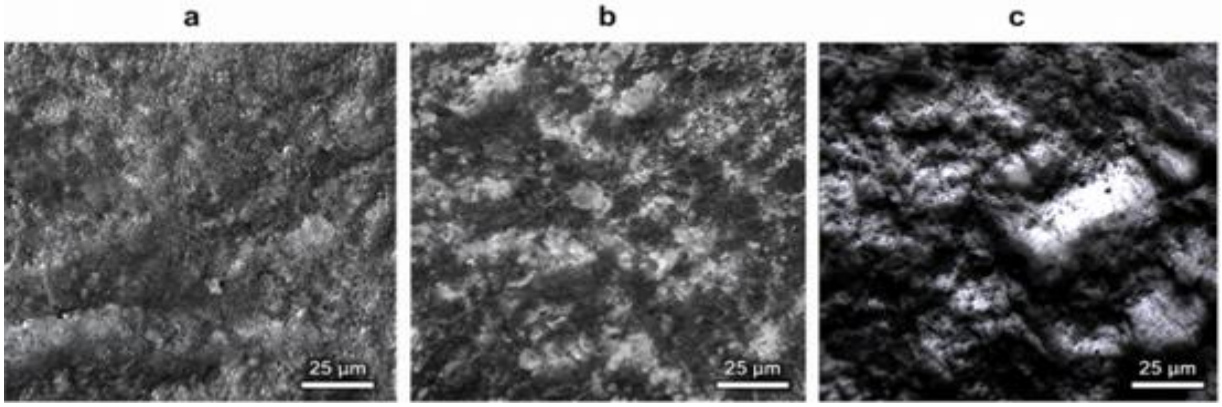


Fig. 16. Optic microscopy images of fracture surfaces after tensile testing: (a) R4V0.2; (b) R80V0.2; (c) flat specimen

The cylindrical specimens have smooth faces, which suggest fast cracks and a failure mechanism dominated by brittleness. On the contrary, the flat specimen has a more rugged surface with bumps and small holes, which suggests a slower failure mechanism with some degree of plasticity before failure.

It can also spot striations and a faceted surface, which are signs that the failure was not instantaneous but rather a gradual accumulation of damage over a period of time. This is consistent with earlier tensile testing, which demonstrated an initial elastic behavior followed by plastic deformation and final failure. It is all consistent with a semi-brittle material such as PVC that is highly dependent on the preparation of the specimens and the local conditions of stress.

So, the analysis of the fractured surfaces is not simply admiring a picture of a fractured material; it is rather a story of the conflict between a brittle failure mechanism and a plastic deformation mechanism operating beneath the surface.

Conclusion

A series of experiments was conducted to investigate the mechanical behavior of PVC, including nonlinear elastic, viscoelastic, and plastic responses. The effects of strain rate, loading rate, and stress triaxiality on deformation and failure were analyzed. Flat and axisymmetric notched specimens were tested to examine the interaction between strain-rate sensitivity and specimen geometry, with a focus on damage evolution.

The main findings of this study are summarized as follows:

1. Strain-rate dependence: As the strain rate increased from 10^{-3} to 10^{-1} s^{-1}, PVC exhibited increased stiffness and yield strength, rising by approximately 15–20 %. This indicates a clear sensitivity of PVC to the rate of loading.
2. Effect of loading rate on flat specimens: higher loading rates led to higher strength and improved ductility. True stress increased from 27.5 MPa at 0.2 mm/s to ~ 34 MPa at 1 mm/s, and true strain at fracture increased from 1.18 to 1.92, showing the significant influence of loading speed on material deformation.
3. Specimen geometry influence: the shape and size of the specimen strongly affected ductility. Specimens with small bend radii (R = 2 mm) displayed limited deformation (true strain < 0.15), whereas larger radii (R = 80 mm) allowed deformation to exceed 0.40, corresponding to over 160 % increase in deformability.
4. Triaxiality effects: Higher stress triaxiality induced earlier onset of cavitation and reduced ductility, whereas lower triaxiality allowed more ductile behavior, highlighting the critical role of multiaxial stress state in PVC failure mechanisms.
5. Fracture surface insights: microscopic observations revealed that fractures initiated from microvoid nucleation, growth, and coalescence. Differences in fracture morphology between flat and notched specimens reflected the combined effects of stress triaxiality and specimen geometry.
6. Implications for design: these experimental results provide a deeper understanding of PVC behavior under various loading conditions, offering valuable guidance for predicting failure and designing reliable polymer components.
7. Future work: further studies will focus on developing a damage model based on these findings to perform predictive simulations under multiaxial loading conditions, enabling more accurate assessment of PVC structural performance.

CRediT authorship contribution statement

Tarek Houari: writing–review & editing, writing – original draft, conceptualization, data curation; **Habib Khellafi**: writing – original draft, conceptualization, investigation; **El Bahri Ould Chikh**: writing – review & editing, conceptualization, investigation; **Hadj Miloud Meddah**: writing–review, editing, investigation; **Mostefa Bendouba**: writing–review & editing; **Mohamed Benguediab**: writing–review & editing, supervision, data curation.

Conflict of interest

The authors declare that they have no conflict of interest.

The authors declare that AI-assisted tools were used only for language editing and grammar correction. All scientific content, analysis, and conclusions are the responsibility of the authors.

References

1. Mohanty AK, Wu F, Mincheva R, Hakkarainen M, Raquez JM, Mielewski DF, Narayan R, Netravali AN, Misra M. Sustainable polymers. *Nature Reviews Methods Primers.* 2022;2: 46.
2. Rai P, Mehrotra S, Priya S, Gnansounou E, Sharma SK. Recent advances in the sustainable design and applications of biodegradable polymers. *Bioresource Technology.* 2021;325: 124739.

3. Mukherjee C, Varghese D, Krishna JS, Boominathan T, Rakeshkumar R, Dineshkumar S, Brahmananda Rao CVS, Sivaramakrishna A. Recent advances in biodegradable polymers: properties, applications and futurs prospects. *European Polymer Journal.* 2023;192: 112068.
4. Khellafi H, Bendouba M, Meddah HM. Experimental and numerical analysis of ductile fracture of polymeric materials. *Transactions of FAMENA.* 2024;48(4): 123–134.
5. Houari T, Benguediab M, Belaziz A, Belhamiani M, Aid A. Fracture toughness characterization of high-density polyethylene using essential work of fracture concept. *Journal of Failure Analysis and Prevention.* 2020;20(1): 315–322.
6. Houari T, Benguediab M, Belaziz A, Kebir T. Numerical Modeling of High-Density Polyethylene (HDPE) Behavior Using Different Fracture Mechanics Approaches. *Annales de chimie - Science des matériaux.* 2020;44: 151–160.
7. Benyerou D, Khellafi H, Meddah HM, Benhamena A, Hachelaf K, Lounis A. Parametric study of spot friction stir welding (FSSW) for polymer materials, case of high-density polyethylene sheets: experimental and numerical study. *Fracture and Structural Integrity.* 2021;15(55).
8. Reddy MI, Kumar MA, Raju CRB. Tensile and flexural properties of jute, pineapple leaf and glass fiber reinforced polymer matrix hybrid composites. *Materials Today: Proceedings.* 2018;5(1): 458–462.
9. Krishnaswamy RK. Analysis of ductile and brittle failures from creep rupture testing of high-density polyethylene pipes. *Polymer.* 2005;46(25): 11664–11672.
10. Saad NA, Al-Maamory MH, Mohammed MR, Hashim AA. The effect of several service and weathering parameters on tensile properties of PVC pipe materials. *Materials Sciences and Applications.* 2012;3(11): 784–792.
11. Adams TM, Hall S, Scavuzzo RJ, Munson D, Andrasik JW, Findlan S. Tensile testing and material property development of high-density polyethylene pipe materials. In: *Proc Int Conf Plast Pipes.* 2008. p.267–274.
12. Tang P, Mo S, Deng N, Tang Y, Hu S. Mechanical behavior analysis and improved phenomenological constitutive model of PVC-UH at various quasi-static strain rates. *Polymer Testing.* 2025;151: 108940.
13. Kiass N, Khelif R, Boulanouar L, Chaoui K. Experimental approach to mechanical property variability through a high-density polyethylene gas pipe wall. *Journal of Applied Polymer Science.* 2005;97(1): 272–281.
14. Günöz A, Kepir Y, Kara M. Tensile strength alteration of glass fiber reinforced polymer (GFRP) composite pipes under seawater-dominated conditions. *Journal of Failure Analysis and Prevention.* 2020;20(4): 1426–1430.
15. Selini N, Guerira F, Tounsi B, Benamara A. Effect of the triaxiality in plane stress conditions: Triaxiality effect in à PVC material. *Engineering, Technology and Applied Science Research.* 2016;6(4): 1082–1086.
16. Mesbah A, Elmeguenni M, Zhu Y, Fahmi Z, Ning D, Jean-Michel. How stress triaxiality affects cavitation damage in high-density polyethylene: Experiments and constitutive modeling. *Polymer Testing.* 2021;100: 107248.
17. Tonkov DN, Kobylyatskaya MI, Vasilyeva ES, Gasumyants VE. Conductive and mechanical properties of graphene-filled polymer composites. *Materials Physics and Mechanics.* 2025;53(2): 48–54.
18. Belaziz A, Mazari M, Bouamama M, Zahaf S, Mouloud D. Experimental study of ductile and fragile pipe cracked in HDPE. *Materials Physics and Mechanics.* 2022;48(2): 199–207.
19. Benyahia H, Tarfaoui M, El Moumen A, Ouinas D, Hassoon OH. Mechanical properties of offshoring polymer composite pipes at various temperatures. *Composites Part B: Engineering.* 2018;152: 231–240.
20. El-Bagory TMAA, Alkanhal TAR, Younan MYA. Effect of specimen geometry on the predicted mechanical behavior of polyethylene pipe material. *J Press Vessel Technol.* 2015;137(6): 061401.
21. Abdoh DA. Three-dimensional examination of tearing fracture mechanism of PVC foams via peridynamics. *Computational Particle Mechanics.* 2025;12: 5095–5109.
22. Djebli A, Bendouba M, Aid A, Talha A, Benseddiq N, Benguediab M. Experimental Analysis and Damage Modeling of High-Density Polyethylene under Fatigue Loading. *Acta Mechanica Solida Sinica.* 2016;29(2): 133–144.
23. Liu J, Yuan R, Sang Q, Dang L, Gao L, Xu B, Xu S. Effect of acetylated citrate plasticizer on mechanical properties of poly (vinyl chloride). *Materials Chemistry and Physics.* 2023;295: 127068.
24. Castagnet S, Deburck Y. Relative influence of microstructure and macroscopic triaxiality on cavitation in semi-crystalline polymers. *Materials Science and Engineering A.* 2007;448: 56–66.
25. Rahimidehgolan F, Magliaro J, Altenhof W. Influence of specimen profile size and thickness on the dynamic compressive behavior of rigid PVC foams. *International Journal of Impact Engineering.* 2023;179: 104676.
26. Akel N, Stoltz G, Wautier A, Nicot F, Touze N. Rate-dependent tensile response of Polyvinyl Chloride geomembranes. *Geotextiles and Geomembranes.* 2025;53: 445–456.
27. Khellafi H, Meddah HM, Ould Chikh B, Bouchouicha B, Benguediab M, Bendouba M. Experimental and numerical analysis of the polyvinyl chloride (PVC) mechanical behavior response. *Computers, Materials & Continua.* 2015;49–50(1): 31–45.

28. Arutyunyan AR. Influence of aging on fatigue and creep properties of polyurethane. *Materials Physics and Mechanics.* 2020;44(2): 112–120.
29. Sasso M, Sarasini F, Mancini E, Lattanzi A, Tirillò J, Sergi C. Experimental characterization and numerical modelling of the impact behavior of PVC foams. *Experimental Mechanics.* 2023;63: 823–837.
30. Ademola AO, Oladele IO, Oluyemi DO, Oke SR, Akinbamiyorin I, Taiwo AS. Development of polyvinyl chloride composites with enhanced mechanical properties using modified ceramic particles. *Iranian Polymer Journal.* 2025;34: 1425–1434.
31. Rahmatabadi D, Soltanmohammadi K, Aberoumand M, Soleyman E, Ghasemi I, Baniassadi M, Abrinia K, Bodaghi M, Baghani M. Development of a pure polyvinyl chloride (PVC) with excellent 3D printability and macro- and microstructural properties. *Macromolecular Materials and Engineering.* 2023;308(5): 2200568.
32. Uddin MA, Wali N, Bashir MT, Sikandar MA, Alsharari F, Alanazi F, Khan MMH, Alshammari TO. Effect of the combination of polyvinyl chloride (PVC) and steel slag waste on the durability and mechanical properties of composite mortars. *Innovative Infrastructure Solutions.* 2024;9: 419.
33. German Institute for Standardization. DIN 8061. *Unplasticized polyvinyl chloride (PVC-U) pipes – General quality requirements and testing*. DIN Standards Committee, 2016.
34. American Society for Testing and Materials. ASTM D638-14. *Standard Test Method for Tensile Properties of Plastics*. West Conshohocken, PA, USA: ASTM International; 2014.